Advances in imaging low-grade gliomas

STEPHEN J. PRICE

Academic Neurosurgery Division, Department of Clinical Neurosciences,
Addenbrooke's Hospital, Cambridge, UK

With 12 Figures and 1 Table

Contents

Abstract

Imaging plays a key role in the management of low-grade gliomas. The traditional view of these tumours as non-enhancing areas of increased signal on T_2-weighted imaging is now accepted as being incorrect. Using new MR and PET techniques that can probe the pathological changes with in these tumours by assessing vascularity (perfusion MR), cellularity and infiltration (diffusion weighted and diffusion tensor MR), metabolism (MR spectroscopy and FDG PET) and proliferation (MR spectroscopy, methionine PET and ^{18}F-fluorothymidine FLT PET). These tools will allow improvements in tumour grading, biopsy/therapy guidance and earlier assessment of the response to therapy.

Keywords: Magnetic resonance imaging; positron emission tomography; prognostic factors; perfusion imaging; diffusion imaging; MR spectroscopy; biopsy guidance; response to therapy.

Introduction

Advances in imaging have been central to advances in managing brain tumours. In low-grade gliomas, however, imaging is probably more important than other brain tumours. They are the major group of tumours where making a diagnosis and start a management plan of 'watch and wait' based purely on imaging [115]. It is essential, therefore, imaging is able to differentiate low-grade gliomas from other conditions, especially the high grade tumours, and that it can identify malignant transformation at an early stage.

The last few years have seen a change in imaging practice. Conventional imaging is excellent at providing information on anatomical location as well as providing valuable information to assist making a diagnosis. New techniques, however, probe pathophysiology by showing features like the tumour's vascularity (perfusion imaging), cellularity and infiltration (diffusion weighted and diffusion tensor imaging) and metabolism (MR spectroscopy and positron emission tomography – PET) [110]. In this review I plan to outline the limitations of conventional imaging techniques and will review the potential role the new MRI and PET imaging techniques may have in the diagnosis and man-

agement of low-grade gliomas (principally WHO Grade II diffuse astrocytomas, oligodendrogliomas and the mixed oligoastrocytomas).

Conventional imaging

Computed tomography (CT) imaging

Low grade gliomas can be difficult to detect on CT as they appear as regions of either low or similar density to normal brain. Calcification is seen in 20% of diffuse astrocytomas and 40% of oligodendrogliomas [74]. Contrast enhancement is not uncommon, and is seen in up to 20% of oligodendrogliomas [74]. This cannot be used to reliably grade these tumours as 31% of 'highly anaplastic' astrocytomas and 54% of 'moderately anaplastic' astrocytomas fail to enhance [17].

Magnetic resonance imaging

As MRI provides better soft tissue resolution, it should be considered the imaging modality of choice: CT should only be used to assess these tumours when MR is contraindicated. An example of the difference in appearances is shown in Fig. 1. On MRI, low-grade gliomas usually appear as well defined masses that are low signal on T_1- and high signal on T_2-weighted imaging and

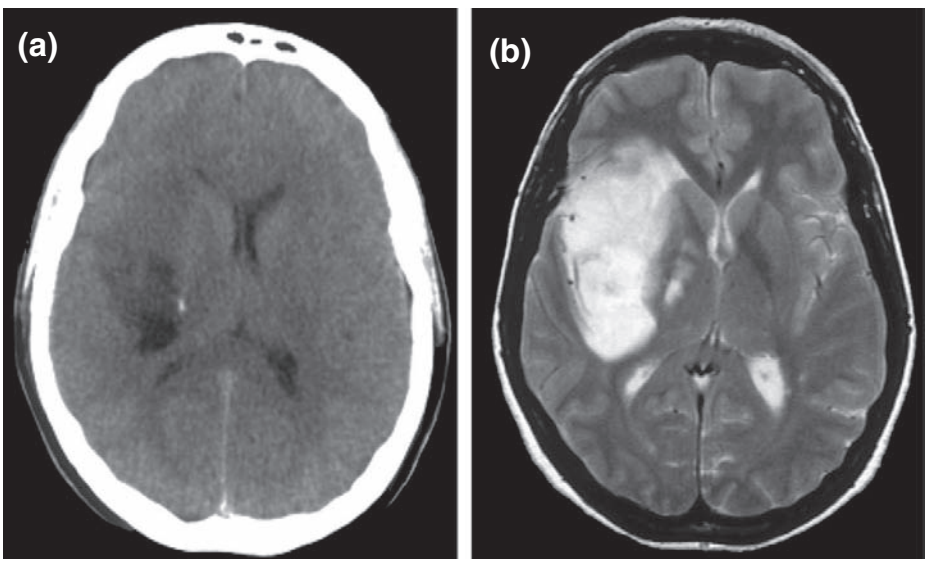

Fig. 1. An example of the difference in appearance between CT and MRI. This 35-year-old male presented with a seizure. The CT (a) shows low density mainly in the posterior part of the tumour. Only the T_2-weighted MRI image (b) shows the full extent of the tumour clearly

produce little mass effect with little oedema [28]. These appearances, however, should not be considered as diagnostic. In a study where patients with these criteria for low-grade glioma underwent a biopsy, the diagnosis was changed in half of cases, with most showing features of an anaplastic glioma, and one having a non-neoplastic condition (encephalitis) [63].

Contrast enhancement in low-grade gliomas

Although low-grade gliomas are considered as non-enhancing tumours, contrast enhancement cannot differentiate between high- and low-grade gliomas. Alokaili *et al.* found that 35% of low-grade gliomas enhanced, and 16% of high grades did not [1]. Other studies suggest that one third of non-enhancing tumours are in fact high grade [123]. For oligodendroglial tumours the situation is more confused with between 50 and 60% of WHO Grade II oligodendrogliomas enhancing [55, 148] while 38% of anaplastic oligodendrogliomas do not enhance [148]. An example of enhancement in a WHO Grade II oligodendrogliomas can be seen in Fig. 2.

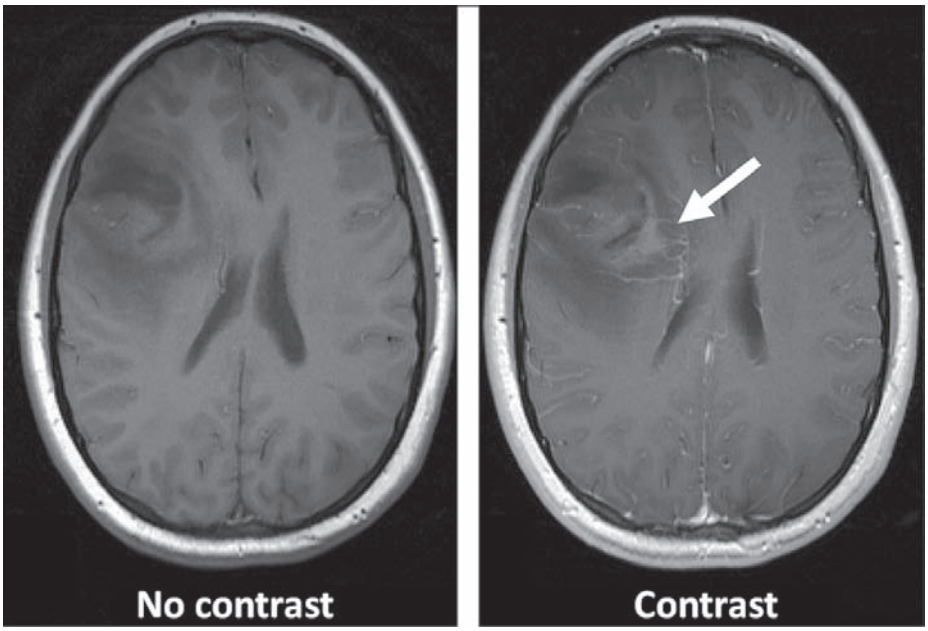

Fig. 2. An example of enhancement in a WHO Grade II oligodendroglioma. This 20-year-old female presented with seizures. Imaging showed a posterior frontal lobe tumour with areas of subtle enhancement mainly on the deep surface (arrowed). She underwent craniotomy and debulking of this lesion which exhibited no evidence of cellular or microvascular proliferation that would suggest it was a more aggressive tumour

Subtle enhancement can be demonstrated using quantitative methods [140]. By calculating the volume of a low-grade glioma that enhances more than 10% compared to the baseline, Tofts *et al.* could show that in some low-grade gliomas the volume of enhancement increased over a number of months before tumour transformation. In tumours that did not transform, the enhancing volume remained stable [140]. The volume of enhancing tissue had prognostic information; tumours with an enhancing volume greater than 4 mLs had a worse prognosis with only 28% of patients progression free at 5 years, compared to 80% of patients with an enhancing volume less than 4 mLs [140].

Assessment of tumour margins with conventional MR

Although low-grade gliomas can appear as distinct masses, it is well appreciated that they can spread beyond the abnormality seen on both T_2- and T_1-weighted imaging [113]. The margin of low grade tumours is usually very indistinct on T_1-weighted imaging and is better demonstrated on T_2-weighted imaging. The use of sequences such as fluid attenuated inversion recovery (FLAIR) – a sequence that typically produces a T_2-weighted image where the signal from CSF is nullified, shows the extent of these tumours very well and often will show subtle abnormalities not appreciated with conventional T_2-weighted images; this is particularly true in regions around the ventricles.

Table 1. *Summary of the differences between astrocytomas and oligodendrogliomas, and the 1p19q status of oligodendrogliomas*

Modality	Astrocytomas vs. oligodendrogliomas	1p19q status
Conventional MRI	Little to differentiate them. Contrast enhancement more common in oligodendrogliomas	LOH of 1p19q is associated with indistinct margin and heterogeneity on T_1 and T_2-weighted imaging
Perfusion MRI	Low rCBV in astrocytomas, increased in oligodendrogliomas	Higher rCBV with LOH 1p19q
Diffusion MRI	Lower ADC in oligodendrogliomas compared to astrocytomas	1p19q loss associated with even lower ADC values
MR Spectroscopy	Larger increase in Cho and Cr in oligodendrogliomas compared to astrocytomas	No difference found
FDG-PET	More marked hypometabolism with astrocytomas	Increased FDG uptake seen with 1p19q loss

rCBV Relative cerebral blood volume; *ADC* apparent diffusion coefficient; *LOH* loss of heterozygosity; *Cho* Choline; *Cr* Creatine; *FDG* fluorodeoxyglucose.

In oligodendrogliomas, studies assessing tumour margin have shown that tumours with indistinct tumour margins are more likely to have loss of heterozygosity at chromosomes 1p19q [55, 87] – an important genetic marker of chemosensitivity and prolonged survival [14]. This genotype of oligodendrogliomas also demonstrated heterogeneous T_1- and T_2-weighted appearances [55]. The suggestion was that the indistinct tumour margin is also a marker of tumour infiltration [87], but image guided biopsies in this group of patients has failed to show this [55]. There is some suggestion that the more indistinct tumour margin is associated with a shorter time to progression and overall survival [38]. These findings are summarised in Table 1.

Assessment of low-grade glioma growth

Changes in low-grade gliomas volume can be assessed by volumetric studies. Follow up of a cohort of oligodendrogliomas and oligoastrocytomas showed that these tumours have a mean growth rate of 4.1 mm/year [80]. Where the diameter grew faster than 8.1 mm/year, the median survival was 5.1 years, compared to more than 15 years where the growth rate was below this threshold [103].

Advanced MRI techniques

Conventional MR methods focus on structural changes within tumours. The last section showed that these are usually non-specific and therefore only provide limited information. Advances in MR technology have allowed faster imaging, at higher fields and create a more homogeneous magnetic field. This has allowed the development of new techniques that probe tumour pathology and are described in more detail in other reviews [110]. Since low grade tumours are classified by the WHO as tumours of increased cellularity without features of anaplasia (i.e. proliferation or disrupted cytoarchitecture), and no increase in vascularity or development of necrosis, imaging methods that can look at changes in cellularity, vascularity and metabolism may allow a better differentiation of low-grade gliomas from both higher grade tumours and more benign conditions. It may also provide prognostic information, identify early transformation and allow better direction of biopsies or other therapies.

Perfusion MRI

One of the key histological features of low-grade gliomas is their lack of microvascular proliferation [61]. The development of endothelial hyperplasia has been shown to be a poor prognostic marker in oligodendrogliomas [25]. Perfusion imaging provides additional information about tumour vascularity.

The relative cerebral blood volume (rCBV) of tumours correlates with tumour vascularity as assessed by non-quantitative scales of histological vascularity [4, 131], measures of microvascular density [5] and angiographic vascularity [131]. It also correlates with the expression of vascular endothelial growth factor (VEGF) within the tumour [77] and the presence of endothelial hyperplasia [15].

Differentiating high- from low-grade gliomas

Many studies have attempted to use perfusion MRI to provide a method to non-invasively grading gliomas [4, 5, 9, 62, 70, 126, 131, 133]; all these studies show that low-grade gliomas have a significantly lower rCBV than glioblastomas (an example in a WHO Grade II astrocytomas is shown in Fig. 3). Attempts to find a threshold that can differentiate between high- and low-grade gliomas have been hampered by the use of different acquisition techniques and methods of reporting the rCBV. Using a spin echo technique that is sensitive to the microvascular component tends to give a lower ratio than using a gradient echo technique [33, 133] that is sensitive to the 'total' CBV from all vessels [8]. Studies using SE sequences suggest that a rCBV threshold of 1.5 can differentiate between high- and low-grade gliomas [4, 75]. Published thresholds for GE sequences are more variable and depend on

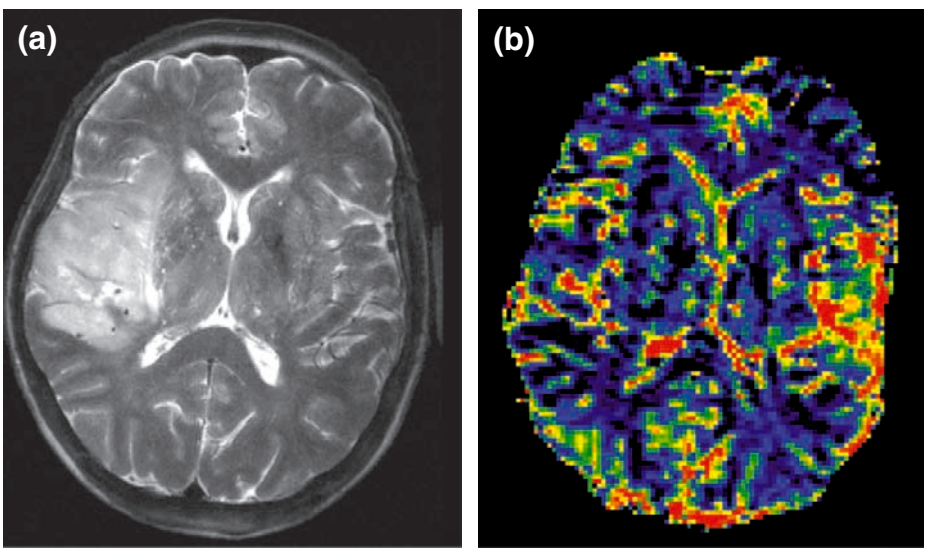

Fig. 3. This 61-year-old female presented with focal seizures affecting her left hand. Imaging (a) showed this to be a non-enhancing lesion in the right insular region. Perfusion imaging (b) showed low rCBV in the tumour (measured at 1.3). Biopsies revealed this to be a WHO Grade II astrocytomas. She remains progression free at 4 years

whether the aim is to increase specificity (rCBV 1.75–2.9) [71, 126] or increase sensitivity (rCBV 3.5) [71].

There are a number of problems using perfusion parameters to grade gliomas for an individual patient. The first is that all studies show marked overlap of rCBV values in different tumour grades [34, 62, 126, 131, 133], particularly differentiating WHO Grade III from either WHO Grade II or WHO Grade IV gliomas. Secondly, most measures are made by placing a region of interest onto the brightest 'hot spot'. This is dependent on the location the region is placed – more reproducible results can be obtained using measures from histogram analysis of the whole tumour [36, 72]. Finally, oligodendrogliomas have higher rCBV values than astrocytic tumours [16, 75] – a finding related to their dense network of branching capillaries that resembles the pattern of 'chicken-wire' (an example is shown in Fig. 4). As a result, low grade oligodendrogliomas could be falsely graded as a higher grade tumour in unselected groups of low-grade gliomas. Studies that only include oligodendrogliomas show a significantly higher rCBV in WHO Grade III anaplastic oligodendrogliomas compared to WHO Grade II oligodendrogliomas [129]. Although this study had small numbers of patients (7 per group) it concluded

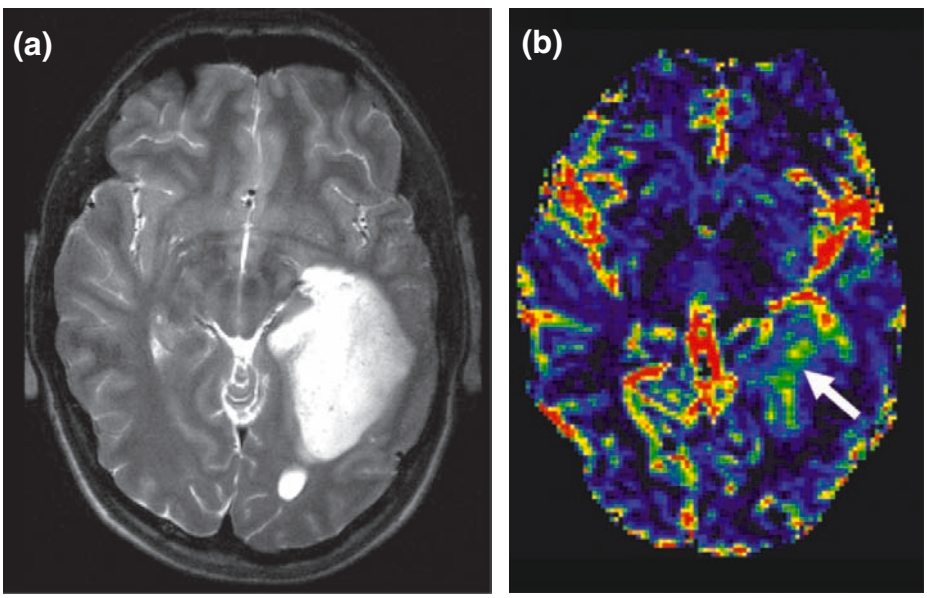

Fig. 4. An example of the increased rCBV seen with oligodendrogliomas. This 18-year-old male presented with a seizure. (a) Conventional imaging showed a large, non enhancing mass adjacent to the atrium of the ventricle. (b) Perfusion imaging showed increased rCBV within part of the tumour (arrowed). This was biopsied and confirmed to be a WHO Grade II oligodendroglioma without any anaplastic features. The patient remains progression free after 3 years

that an rCBV threshold of 2.16 could differentiate between the grades with 100% specificity and 86% sensitivity. The rCBV in oligodendroglial tumours is further complicated by the fact that tumours with chromosomes 1p19q deletion have an even higher rCBV [58, 68] (cf. Table 1).

Perfusion imaging as a prognostic marker in low-grade gliomas

Since perfusion MR can identify areas of microvascular proliferation, a known histological feature of poor prognosis, attempts have been used to use perfusion MRI to assess prognosis. Law *et al.* have shown that an rCBV threshold of 1.75 could differentiate between a prolonged survival group (median time to progression approx. 10 years) with a poor prognosis group (median time to progression less than one year) [69, 73]. An example of this is shown in Fig. 5. A recent follow up study has shown that there is a significant increase in rCBV that can be detected up to one year before there was evidence of tumour transformation [24].

Perfusion MR has also been used to guide biopsies of non-enhancing tumours [78]. Where perfusion MR demonstrated heterogeneous rCBV, the

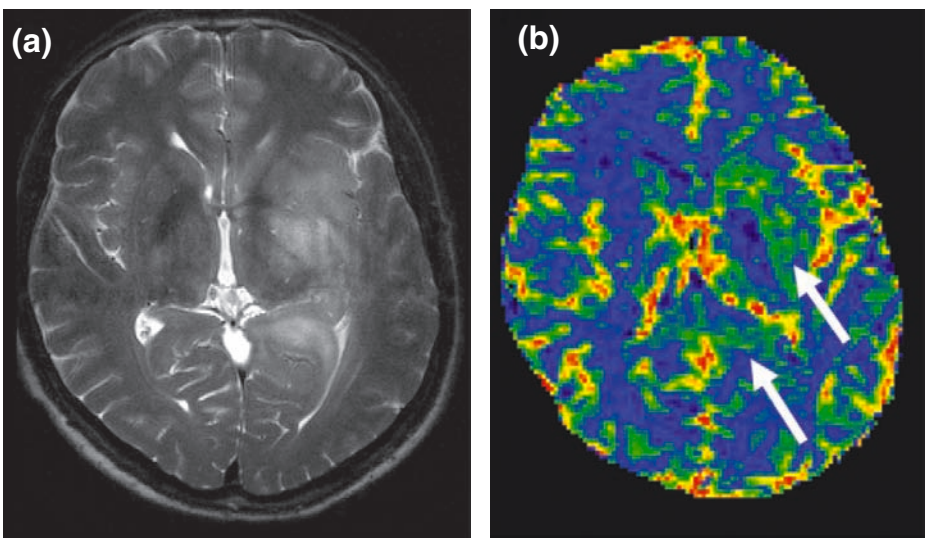

Fig. 5. This 45-year-old male who presented with seizures and headache was shown to have a non-enhancing tumour in the left insular region extending along the temporal lobe to the atrium of the lateral ventricle (a). Biopsies confirmed it to be a WHO Grade II astrocytoma. In contrast to the patient presented in Fig. 3, perfusion imaging (b) shows areas of increased rCBV (measured at 2.8 – arrowed). Post-biopsy he had radiotherapy (54 Gy in 30 fractions). Within one year he clinically deteriorated and had evidence of tumour progression and the development of enhancement on imaging. He died of progressive disease despite chemotherapy 18 months after initial presentation

target for biopsies was taken as the region with the highest rCBV. Biopsies of these regions demonstrated oligodendroglial differentiation or anaplastic regions whereas tumours with uniformly low rCBV were more likely to be WHO Grade II diffuse astrocytomas.

Perfusion imaging at recurrence: differentiating radiation necrosis from recurrent tumour

One major difficulty in the management of all patients with brain tumours treated with radiotherapy is differentiating changes that occur following treatment. Tumour recurrence and radiation necrosis can appear similar and both can have a very variable appearance on conventional MRI [18]. Radiation necrosis can be identified by areas of reduced rCBV. Studies in patients with radiation necrosis in the temporal lobes following radiotherapy of nasopharyngeal carcinomas (where there is no confusion with recurrent tumour) showed reduced rCBV in these regions [143]. Subsequent studies have suggested that rCBV values below 0.6 are predictive of radiation necrosis, and values above 2.6 are predictive of tumour; the difficulty lies with the mixed cases with values between 0.6 and 2.6 [134].

Diffusion-weighted and diffusion tensor MRI

The appearance of low-grade gliomas on diffusion-weighted (DWI) imaging is variable. The high signal on DWI images is largely a result of T_2-weighted 'shine through' effects and is more dependent on the T_2-weighted appearance [91]. The increase in the apparent diffusion coefficient (ADC) is therefore used as a better, quantitative marker of diffusion in brain neoplasms.

ADC values are determined by a combination of processes. Firstly, it is increased by the increased volume of water in the tumour tissue due to vasogenic oedema. The ADC value correlates with both oedema (using T_2-weighted signal intensity) and blood brain barrier permeability (using the percentage enhancement seen on T_1-weighted imaging following a dose of gadolinium contrast) [95]. In addition, the ADC is dependent on cellularity – the more cells present, the less the distance that the water molecules can diffuse. Studies have indeed confirmed that there is an inverse correlation between ADC and tumour cellularity [40, 65, 132].

Grading gliomas using diffusion-weighted imaging

As low-grade gliomas tend to be less cellular than their high grade counterparts, attempts have been used to grade gliomas using ADC values. Studies suggest low-grade gliomas have a significantly increased ADC compared to high grade tumours [65, 132].

The problems of using ADC values to grade these tumours are similar to the use of perfusion MRI. There is marked overlap in individual values making grading of individual patients impossible. In addition, it is not possible to differentiate between low-grade gliomas and other benign problems [12], and some studies that have largely used WHO Grade III tumours as their high grade tumours could not differentiate between high- and low-grade gliomas at all [67]. In addition, just like using rCBV measures, ADC is significantly lower in oligodendrogliomas [141], and within the oligodendrogliomas the tumours that have lost chromosome 1p19q have lower ADC values [56]. These changes, however, are much less marked than the changes seen in rCBV values (cf. Table 1).

Some studies have used diffusion-weighted imaging to differentiate radiation necrosis from tumour recurrence following therapy. Areas of tumour recurrence showed higher mean ADC values compared to radiation necrosis [48, 135]. Unfortunately the values for necrosis and recurrence overlap making it of little value for the individual patient. Compared to other modalities, diffusion imaging does not appear to add much in this setting [120].

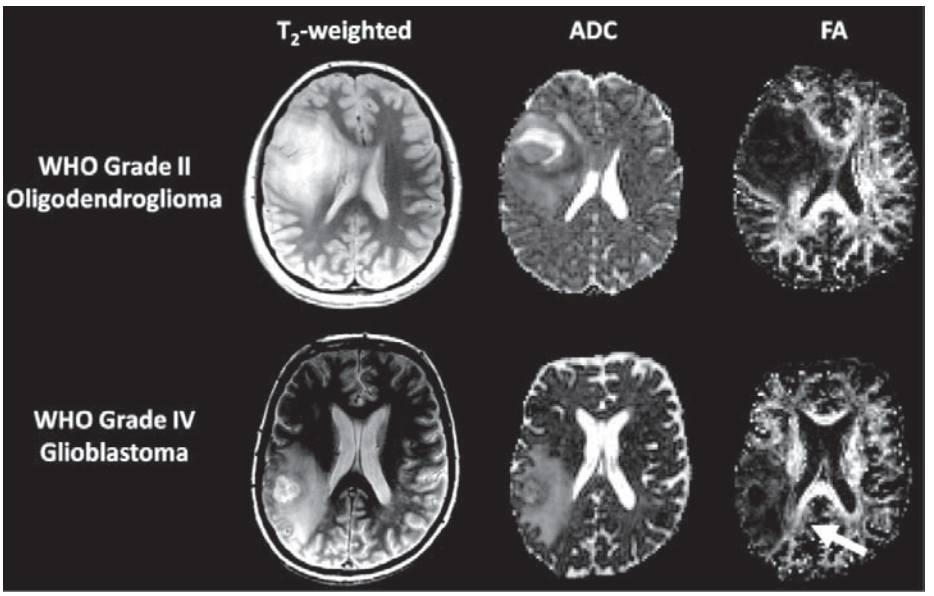

Fig. 6. Diffusion weighted (ADC) and diffusion tensor (FA) in a patient with a WHO Grade II oligodendrogliomas (top row) and WHO Grade IV glioblastoma (bottom row). The lower grade tumour shows regions of much higher ADC and generally lower FA compared to the glioblastoma. In the glioblastoma patient there is infiltration of the adjacent white matter tracts which is seen as gradual reduction in FA values in these regions (arrowed). This is not seen in the low grade patient

Diffusion tensor imaging in low-grade gliomas

Diffusion tensor imaging (DTI) is a modification of DWI that is sensitive to the directional diffusion of water (anisotropy). It provides more information on tissue architecture that is not available on DWI as reduced anisotropy can occur with loss of tissue organisation (e.g. as seen with demyelination), destruction of axonal processes, widening of extracellular spaces (e.g. as seen with tumour infiltration) and changes in cell size. The most commonly used parameter of DTI imaging is *fractional anisotropy* (FA) – a rotationally invariant measure of anisotropy.

Studies in tumours show that the FA values correlate with tumour cellularity and vascularity [7] as a result low-grade gliomas tend to have lower FA values. Using a threshold of 0.188, Inoue *et al.* could differentiate between high- and low-grade gliomas [52]. Studies looking at the periphery around the tumour have shown there is no reduction in FA in the white matter tracts adjacent to low-grade gliomas, compared to the reduction in normal appearing tracts adjacent to high-grade gliomas [43, 111] (Fig. 6). This difference has been suggested as due to tumour infiltration – but since low-grade gliomas infiltrate, especially oligodendrogliomas, it probably relates to white matter destruction from tumours and the lack of sensitivity of these DTI measures. Recent biopsy studies using novel tissue signature methods [106, 114] have shown that DTI can identify this occult infiltration, even in low-grade gliomas [113].

Magnetic resonance spectroscopy

Unlike the other imaging methods, MR spectroscopy (MRS) allows the non-invasive study of metabolism from either a single, small region of interest (single voxel spectroscopy) or multiple regions (multivoxel or chemical shift imaging). Virtually all clinical spectroscopy studies focus on the ^{1}H nucleus (which is essentially a proton) due to its abundance, its strong magnetic signal and the fact it can be detected using standard MR equipment. Although up to 30 peaks can be identified in the ^{1}H spectrum, fewer peaks are commonly studied in clinical practice.

MR spectroscopy to differentiate high- and low-grade gliomas

All gliomas show a spectrum with an increased choline (a marker of membrane turnover) and reduced N-acetyl aspartate (NAA – a neuronal marker) (Fig. 7). Peaks of lipid (a marker of necrosis) and lactate (a marker of tumour hypoxia) are rarely elevated in low-grade gliomas, but are elevated in higher grade gliomas [84, 90, 93, 97, 98] (Fig. 8). Their presence in low-grade gliomas appears to mirror the proliferative index; when the Ki67 labelling index is <4% no lipid or lactate is detectable, when it is 4–8% lactate can be detected without lipids and

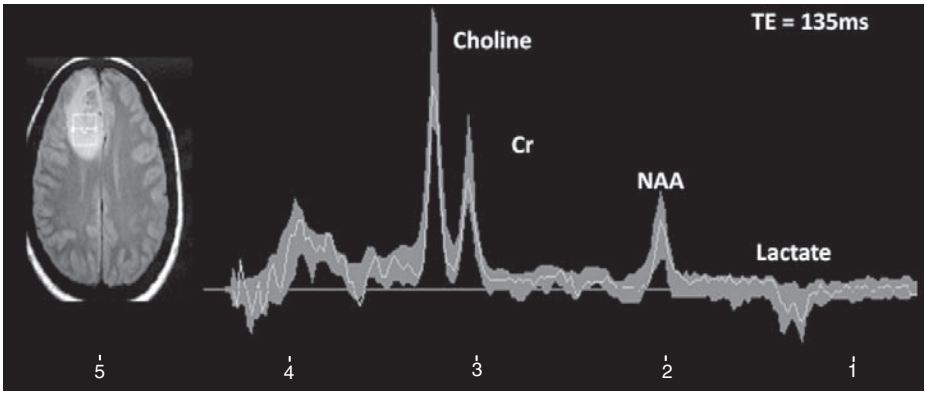

Fig. 7. Single-voxel, proton spectra from 20 patients with WHO Grade II astrocytomas (solid line is mean, grey area is standard deviation). There is an increase in choline peak with reduction of NAA (which still can be seen). Lactate, with this long echo time ($TE = 135$ ms) is frequently seen in these patients as an inverted peak

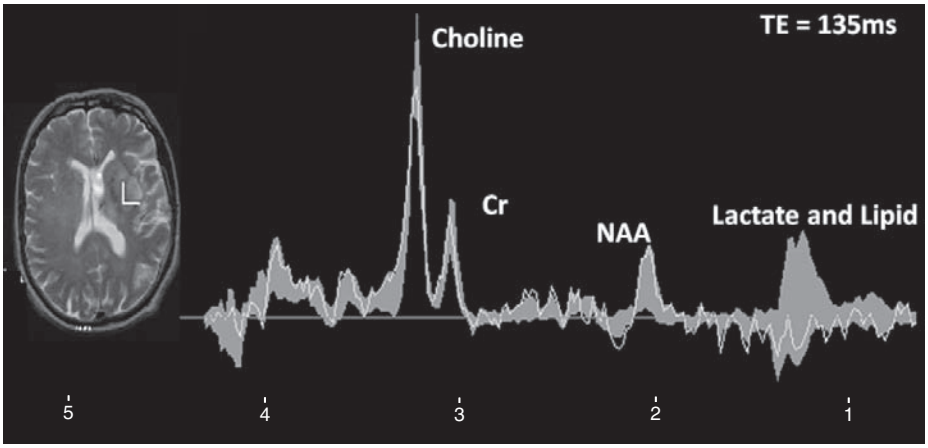

Fig. 8. Mean spectra (with standard deviation) for five patients with WHO Grade III anaplastic astrocytomas. Compared to Fig. 7 there is a higher choline peak with more reduced NAA. Lipids and lactate can now be seen regularly

above 8% there is an increase in lipids [46]. Although creatine (Cr – a marker of energy metabolism) is often used as a reference signal to express the other peaks as a ratio to the creatine peak, it is actually decreased in brain tumours [88, 90]. The reduction is, however, small and does not appear to be related to the grade of tumour [90].

One problem with MRS is that tumours are heterogeneous. Single voxel techniques have the same problems with sampling error that is seen with biopsies. Multivoxel techniques can over come this, and 3D techniques are

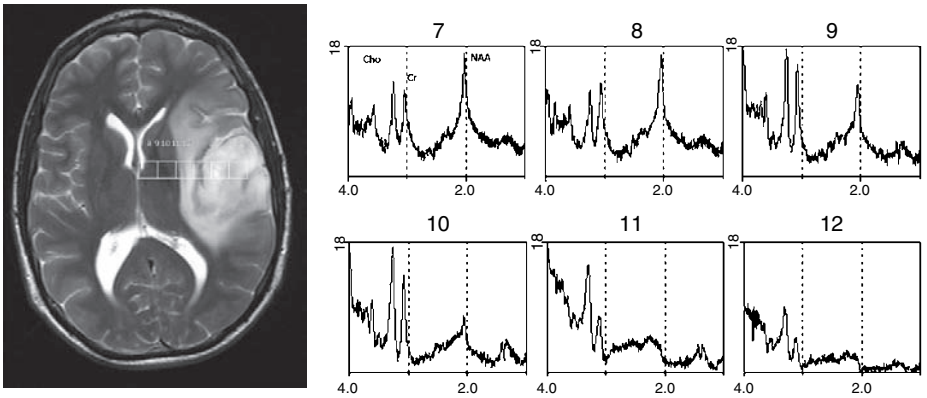

Fig. 9. Multivoxel spectra from a 16×16 grid at TE 30 showing variation in NAA, creatine and choline going from normal brain (in voxel 7) to pure tumour (in voxels 11 and 12).

becoming more widespread. An example of the heterogeneity of spectra across a low-grade glioma is seen in Fig. 9.

Various studies have tried to understand what the MRS findings tell us of the tumour biology. McKnight *et al.* have shown that the Choline/NAA ratio correlates with cell density, proliferative index and the ratio of proliferation to cell death [86]. Other groups have also shown that the Choline/NAA and Choline/Cr correlate with the proliferation index and that the normalised values of Choline correlate with both proliferation index and cell density. In a cohort of low-grade gliomas Guillevin *et al.* showed that cellular atypia correlated with increased Choline/NAA ratio, a lower NAA/Cr ratio and the lipid peak [46].

Using this information it can be shown that low-grade gliomas have a significantly lower Choline/Cr ratio [71, 84, 93, 97, 98, 128], and an increase in NAA [71, 85, 93, 97, 98, 128]. It is possible to differentiate between high- and low-grade gliomas with sensitivity of 73–92% and specificity of 63–100% [6, 37, 51, 71, 124]. Studies comparing the performance of MR spectroscopy and perfusion imaging to correctly grade tumours provide mixed results. One study suggested spectroscopy was superior to perfusion [37], while another showed rCBV measurements were better, and the addition of metabolic information did not improve the diagnostic yield [71].

Differentiating low-grade gliomas from other conditions

MRS has a role in differentiating low-grade gliomas from other conditions that can present with similar clinical symptoms and appearances on conventional imaging. Focal cortical developmental malformations (e.g. cortical dysplasias and dysembryoplastic neuroepithelial tumours) certainly have very similar con-

ventional imaging findings. Vuori *et al.* showed that low-grade gliomas had a more marked reduction in NAA and increase in Choline, while the focal cortical developmental malformations exhibited less change (< 30% difference to normal brain) [146]. The NAA/Cr ratio, in particular, was markedly lower in low-grade gliomas than in the focal cortical developmental malformations. Tumefactive demyelinating plaques, however, have similar MRS appearances to low-grade gliomas with increase in choline, reduced NAA and can contain lactate. Repeat imaging after an interval shows the spectra returns to a more normal appearance in MS, but remains abnormal in low-grade gliomas [13].

Most of the studies discussed so far have concentrated on peak height of a very limited number of metabolites. A recent multicentre study – the INTERPRET study (International Network for Pattern Recognition of Tumours Using Magnetic Resonance – *http://azizu.uab.es/INTERPRET/index.html*) developed a computer-based decision support system that analysed the whole spectrum as a tool to assist with diagnosis. Their database could correctly classify brain lesions in 89% of cases and has provided an infrastructure for other multicentre studies [137]. The eTUMOUR project (www.etumour.net) aims to further develop the database to provide more information to improve differentiation of tumours that may appear similar on conventional imaging.

Identification of low-grade glioma subtypes with MR spectroscopy

Just like diffusion and perfusion MR, there are differences in the MRS spectrum that can differentiate low-grade astrocytomas from oligodendroglial tumours. Oligodendrogliomas exhibited a more marked increase in choline and an increase in creatine. This is in contrast to astrocytomas where there is a more modest increase in choline and a decrease in creatine [146]. Analysis of the whole spectrum could also differentiate between these types of tumours [137]. Unlike perfusion and diffusion imaging, however, spectroscopy cannot differentiate between tumours with or without loss of chromosomes 1p19q [57] (cf. Table 1).

MRS to detect low-grade glioma transformation

Since high-grade gliomas can be differentiated from lower grade tumours by their larger increase in Choline and decrease in NAA and the presence of lactate and lipid, attempts have been made to use these features to identify transformation in low-grade gliomas. One of the difficulties in using MR spectroscopy for follow up studies is the small region that is imaged in single voxel spectroscopy – it is very possible the voxel is not located in the region of the tumour where transformation occurs. Attempts to monitor tumours using this method had a specificity of only 57.1% [3]. Even using multivoxel imaging

techniques appears to have limited uses. Tedeschi *et al.* showed that progressive tumours had a markedly increased (>45%) Choline compared to stable tumours, but it did not appear before they could identify progression on conventional imaging [138]. Reijneveld *et al.* found that in their seven progressive patients, MRS could only detect a difference before conventional MR in 2 cases, and in 2 patients they failed to show any progression on MRS [116]. More worryingly, four of their seven patients with stable disease showed progression on MRS.

Using MRS to assess response to therapy in low-grade gliomas

As a tumour responds to chemotherapy changes in cell numbers/density can occur before there is obvious change in tumour volume. As most studies report little change in tumour volume, there is great interest in using advanced imaging methods to detect early response to therapy. Murphy *et al.* showed in a group of 12 patients with low-grade gliomas treated with temozolomide the decrease in the choline peak correlated with a reduction in tumour volume [94]. They suggested this was due to reduced cell density. They found some increase in NAA, but this was only seen in 3 patients. A further case study that combined MRS with DTI also reported a decrease in choline and an increase in NAA [127]. The decrease in choline correlated with increases in ADC – further evidence that it is due to reduced cellularity. The increase in NAA also correlated with increases in FA suggesting improvement in axonal structures. Further studies are needed to monitor treatment response in individual patients.

One of the major uses of MRS in a clinical setting is the differentiation of radiation necrosis from tumour recurrence. Regions of radiation necrosis exhibit lower NAA/Cr and NAA/Cho ratios and higher Cho/Cr ratios than tumour progression [19, 119]. The presence of lactate can be seen with either pathology and suggests that ischaemia is the underlying mechanism of radiation injury [19]. Like the other modalities, although MRS can identify pure tumour and pure radiation necrosis, it is not able to differentiate the mix picture, which is probably the most common setting [119].

^{31}P-Phosphate MR spectroscopy in low-grade gliomas

Although ^{1}H-proton spectroscopy is the most used clinically, ^{31}P-phosphate spectroscopy can also be performed, with the appropriate equipment. It can provide information on both phosphate metabolites (especially ATP and energy metabolites) and pH. Studies with low-grade gliomas show that they have a similar phosphorus spectrum to normal brain, with essentially normal pH values [49, 79]. The development of anaplastic changes results in a decrease in both phosphocreatine and phosphodiesters peak, with pH showing increas-

ingly alkaline values [49, 79]. With treatment there is a trend to increasingly alkaline pH values, but studies have been done on limited patient numbers and it is difficult to define a relationship with prognosis [79].

Positron emission tomography (PET) imaging

Over the last decade PET imaging has developed with our improved knowledge of cellular biochemistry and the development of new radiotracers that can probe these biological processes. The multiple pathways involved in tumour development can now be studied by these processes. Although a number of PET tracers have been developed for cancer imaging, only three groups are in routine clinical usage. These study glycolytic metabolism, protein synthesis and nucleotide uptake as markers of tumour proliferation. Newer tracers that study membrane turnover have been developed but their use has yet to be determined.

Imaging glycolytic metabolism: 2-[^{18}F]-fluoro-2-deoxy-D-glucose (FDG) PET

It has long been recognised that tumour cells have an increase in glucose utilisation and glycolytic metabolism. Otto Warburg first noticed the relationship between aggressive tumour behaviour and increased glycolysis [147]. It is due to an increase in the expression of numerous genes and is regulated by the hypoxia inducing factor HIF-1. In many tumours there is induction of HIF-1 due to disruption of its normal control that can occur in the absence of hypoxia. The hyperglycolysis seen in tumours is due to increases in glucose transport across the blood brain barrier and cell membranes (e.g. the glucose uptake transporters GLUT-1 and GLUT-3) and increases in the principal enzymes of glucose metabolism (e.g. hexokinase, phosphofructokinase, lactate dehydrogenase and pyruvate dehydrogenase).

The fluorinated glucose analogue 2-[^{18}F]-fluoro-2-deoxy-D-glucose (FDG) has high sensitivity (although poor specificity) for identifying areas of increased tumour metabolism. FDG uptake and metabolism in normal and tumour cells are shown in Fig. 10.

Low-grade gliomas tend to have the same or lower uptake to normal grey and white matter, whereas high-grade gliomas tend to exhibit increased uptake of FDG [31, 136]. Using a tumour-to-white matter ratio >1.5, and tumour-to-grey matter ratio >0.6 it is possible to differentiate high and low grade tumours with a sensitivity of 94% and specificity of 77% [29]. FDG uptake appears to predict grade better than appearances on contrast enhanced CT [104]. In low-grade gliomas areas of increased FDG uptake correlate with tumour anaplasia [44]. Levivier *et al.* found that FDG PET could identify targets for stereotactic

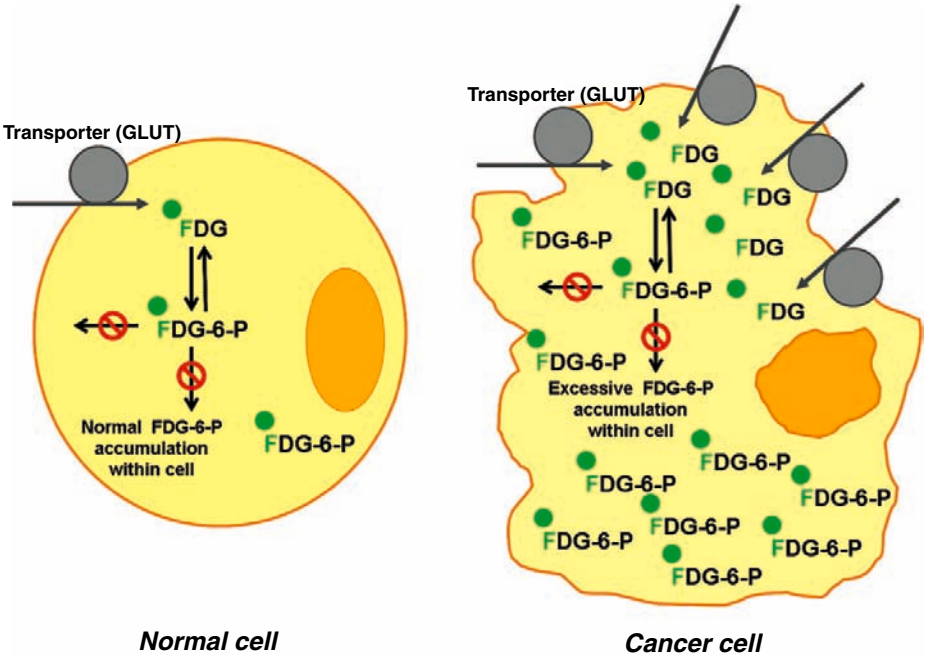

Fig. 10. FDG metabolism in normal and cancer cells. FDG is taken up into cells due to the upregulated glucose transporters (e.g. GLUT-1 and GLUT-3) and is then phosphorylated by hexokinase to FDG-6-phosphate. This does not undergo further enzymatic reactions and, because of its negative charge, it accumulates within the cell

biopsies far better than contrast enhanced CT [76]. They found that 6/35 targets selected by CT were non-diagnostic, whereas 0/55 targets selected by FDG PET were non-diagnostic. Follow up studies suggest that it might be possible to detect the transformation of low-grade gliomas to a higher grade with FDG PET before anatomical changes appear on CT [89, 121].

Studies that have looked at differences in FDG uptake in different histological subtypes of low-grade gliomas suggest that low grade astrocytomas have a lower glucose metabolism than oligodendrogliomas [31]. In series that just look at oligodendrogliomas, FDG uptake is significantly lower in WHO Grade II oligodendrogliomas than anaplastic oligodendrogliomas [30]. Increased glucose metabolism was also seen in low grade oligodendrogliomas with loss of 1p19q heterogeneity [130]. Those with intact chromosomes 1p19q all had reduced FDG uptake (cf. Table 1).

Since increased glycolytic metabolism appears to be a marker for and promoter of a more aggressive phenotype, FDG PET has been investigated as a prognostic marker. The survival of patients with hypermetabolic tumours is worse than those with hypometabolic tumours [2, 27, 105]. Follow up studies suggest increased glucose metabolism may predict tumour transformation [89].

Currently, one of the main uses of FDG PET is the differentiation of recurrent tumour from radiation necrosis. As both will enhance with contrast, standard MR techniques cannot differentiate between these two problems. Recurrent tumours have increased metabolic activity whereas areas of radiation necrosis are hypometabolic [32]. FDG can differentiate between these two with a sensitivity of 75% and specificity of 81% [20]. MR coregistration improves the sensitivity of FDG as it can distinguish recurrence uptake in the normal adjacent cortex. It can be misleading, however, as increased activity can be due to accumulation of activated macrophages.

The real limitation using FDG to assess brain tumours is that the uptake is non-specific and can occur in any region with an increase in metabolic activity. In the normal brain the cortex, basal ganglia, thalami, cerebellum and brainstem have increased uptake, whilst white matter and CSF have low uptake. The uptake is also non-specific since other inflammatory diseases can exhibit increased FDG uptake. In addition, FDG PET is a marker of glycolytic metabolism and not cellular proliferation. Studies have confirmed that the correlation between FDG uptake and Ki-67 expression of tumours is poor [21, 59]. FDG uptake does, however, show a regionally specific correlation with tumour vascularity [5]. The information it provides is therefore complementary to other imaging techniques.

Imaging protein synthesis: amino acid PET studies

In all cancer cells there is an increase in amino acid uptake due to both an increased demand for amino acids due to increased protein synthesis, and an increase in the transport of amino acid as a result of the malignant transformation [53].

Most amino acid labelling studies have used ^{11}C since it does not change the chemistry of the molecule. ^{11}C-methionine (L-[methyl-^{11}C]-methionine) or ^{11}C-tyrosine (L-1-[^{11}C]-tyrosine) are the most commonly used amino acids. The major draw back of using ^{11}C, however, is its short half life of only 20.4 min which means production has to be made when it is required, in a unit with an on site cyclotron. This is in contrast to ^{18}F compounds that have a half life of 109 min that can be produced in a central cyclotron and transported to a number of units for use later in the day. Currently there is much interest in the use of *O*-2-[^{18}F]fluoroethyl-L-tyrosine (FET) as a PET tracer.

In vitro studies have shown good correlation between methionine uptake and cellular proliferation markers [66], a finding confirmed in a cohort of patients who underwent glioma resection [60]. In comparison to FDG PET, methionine PET appears to provide better delineation of tumours [100, 145]. In tumours that are iso-/hypometabolic to glucose, 90% have increased methionine uptake [23]. Low-grade gliomas commonly show methionine accumu-

lation [101], although quantitative values are usually similar to that of normal brain [31]. The uptake in low grade oligodendrogliomas, however, appears to be greater than that of low grade astrocytomas [30, 31]. As the tumour grade increases methionine uptake increases in a more heterogeneous pattern [30, 101]. Methionine PET has a 97% sensitivity for detecting high grade and a 61% sensitivity for detecting low-grade gliomas [101], and it appears to be a more sensitive marker than FDG [30, 41]. Overall, Herholz *et al.* found that in a series of 196 patients, ^{11}C-methionine PET could differentiate low-grade gliomas from non-neoplastic problems in 79% of cases [50]. As there is little uptake into inflammatory cells, methionine appears to be particularly sensitive in differentiating radiation necrosis from recurrent tumour [139], and tumours from inflammatory lesions.

As a prognostic marker, WHO Grade II and Grade III gliomas have a shorter survival time if they exhibit increased methionine uptake [26]. Similar results have been reported using FET [38] This survival prediction is true for both low grade astrocytomas [99] and oligodendrogliomas [117, 118]. Follow up studies show that low-grade gliomas undergoing malignant transformation show increased methionine uptake [121]. Tumours that show stable or reduced methionine following radiotherapy have a more favourable outcome [99].

Since methionine uptake appears to correlate with proliferation and is increased in the higher grade areas, various groups have used it to guide image-guided brain biopsies. Go *et al.* described cases where biopsies taken from areas of increased uptake of L-[1-^{11}C]Tyrosine provided better diagnostic yield than conventional MRI in lesions that did not enhance with gadolinium [42]. Goldman *et al.* compared targets determined from FDG PET with methionine PET and found that methionine could differentiate active tumour from necrosis better than FDG. This group has subsequently shown that combining MRI and PET for biopsy targeting improves the diagnostic yield in brainstem tumours [81], paediatric brain tumours [109] and in tumours with little uptake of FDG [108]. They have also suggested that PET-guided resections could remove the part of the tumour with the largest potential for transforming into a more malignant form, although they have not presented any data that this affects clinical outcome [107].

Imaging DNA synthesis with labelled pyrimidine analogues

Since thymidine is only incorporated into DNA and not RNA it has long been used as a measure of DNA synthesis and is an obvious target for labelling for PET studies. Cells obtain thymidine from both a *de novo pathway* that synthesises thymidine from glutamine and a *salvage pathway* where exogenous thymidine is transported to the cells and is then phosphorylated by

thymidine kinase to thymidine monophosphate. In all cells the de novo pathway provides most of the thymidine used in cells, although there is some evidence, however, that the brain may be deficient in the de novo pathway [39]. Since the ratio of both pathways is relatively constant, there is a constant fraction of thymidine derived from the salvage pathway.

Initial attempts at pyrimidine imaging used ^{11}C-thymidine. This is challenging to produce, involves the short lived ^{11}C isotope and is broken down into metabolically active metabolites. Initial studies in gliomas showed that in half of patients studied the information derived was significantly different in some way from either FDG PET or conventionally MRI [35]. Active tumour could be identified in areas demonstrating little FDG uptake, and within the non-specific area of enhancement on MRI within the tumour bed.

3′-deoxy-3′-fluorothymidine (FLT) was initially developed as an antiretroviral drug. In vitro studies of FLT metabolism have shown that it enters cells using the nucleoside transporters but at half the rate of thymidine [64]. FLT is a selective substrate for TK-1 and it is phosphorylated by TK-1 to FLT monophosphate (FLTMP), again at a rate slower than thymidine [92]. The metabolism of FLT is shown in Fig. 11. As the rate of TMPK is 23-times slower than TK-1 [45] FLT accumulates greater than thymidine in proliferating cells [125]. The small amount of FLTTP produced is not incorporated into DNA due to the modification at the 3′ site.

Clinical validation studies of this model have been performed in patients with lung tumours and has shown that FLT uptake values obtained from compartmental analysis correlate with Ki67 expression in resected tumour specimens [96]. More detailed kinetic analyses in gliomas suggest that although the trapping of FLT-MP by *thymidine kinase*-1 is involve, the most important factor determining FLT accumulation was the rate of transport into the cell [54].

For gliomas a few studies have been recently reported. FLT uptake is markedly increased in high-grade gliomas [21, 22, 54, 112]. Low grade gliomas frequently show no FLT uptake [112] (see Fig. 12). For patients where

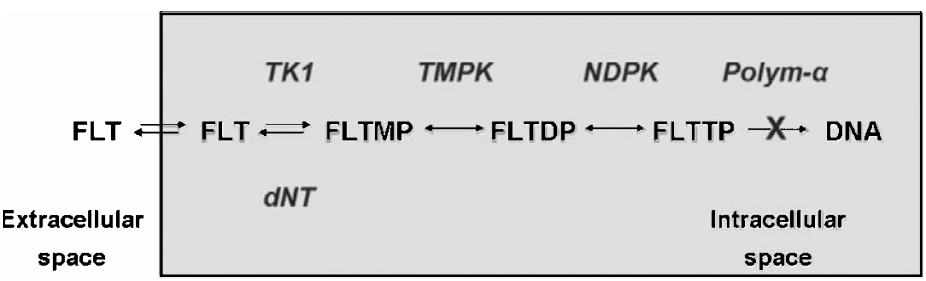

Fig. 11. FLT metabolism in cells. In dividing cells the uptake of FLT is increased. The main metabolism of FLT involves phosphorylation to FLT-MP which is only slowly metabolised further. As a result it accumulates in dividing cells

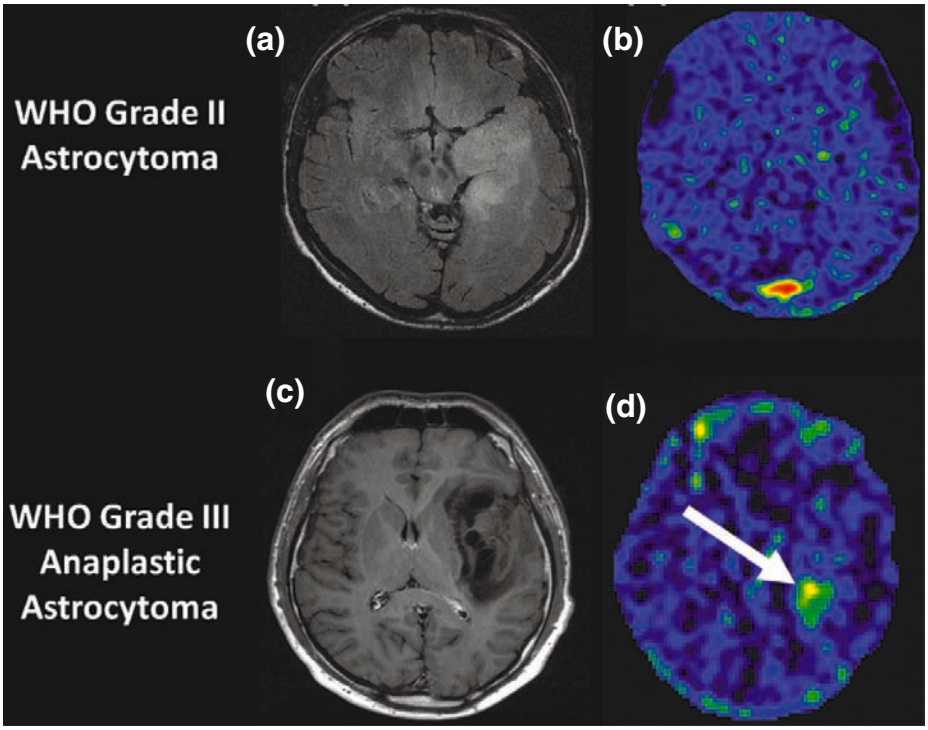

Fig. 12. FLT images in two patients. The upper row shows the FLT in a patient with a WHO Grade II astrocytoma (a). The FLT image (b) shows some uptake in the skull bones and within the sagittal sinus posteriorly. There is no obvious uptake into the tumour. In the lower row this tumour did not enhance with contrast (c). FLT, however, shows a region in the posterior aspect of the tumour that has increased FLT uptake (d). Biopsies were taken from this region which showed anaplastic features sufficient for a diagnosis of WHO Grade III anaplastic astrocytomas

histological material was available, the maximal FLT uptake correlates with the highest MIB-1 labelling index in the tumour [21, 22, 54]. Uptake appears to be a good predictor of tumour progression and overall survival [21]. Compared to FDG PET, FLT is more a sensitive in detecting tumour due to the improved contrast-to-background ratio [21, 22]. False positive results, however, can occur as increased uptake can occur in regions of blood brain barrier disruption – this especially occurs in recurrent low grade tumours following radiotherapy [122].

Imaging hypoxia

One of the main drivers of a 'high-grade' phenotype is hypoxia. A number of markers have been developed for this purpose. Most work has used ^{18}F-fluor-

omisonidazole (^{18}F-FMISO), a nitroimidazole derivative whose metabolites accumulate in hypoxic cells. PET studies have shown that it accumulates in high grade tumours [10, 144] and can differentiate it from other tumours where hypoxia is less of a problem [11]. Studies are needed in low-grade gliomas.

One problem with ^{18}F-MISO is that it is only taken up into viable cells – it will not identify necrotic areas. A promising new marker ^{60}Cu-diacetyl-bis(N^4-methylthiosemicarbazone) (^{60}Cu-ATSM) overcomes this issue. Although studies have been done in man, no studies have yet reported on its use in brain tumours [102].

Imaging membrane turnover

As we have previously seen with MR spectroscopy, imaging membrane turnover correlates with cellular proliferation. Two different PET approaches have been used for this. The first, like proton spectroscopy, uses choline. Although both ^{11}C and ^{18}F based tracers have produced, the fluorinated version has a higher tumour-to-normal ratio [47]. In low-grade gliomas the uptake is low – similar to normal brain. More aggressive/more anaplastic areas within a glioma show increased uptake and, as a result, may guide biopsies [47].

The second method uses 1-^{11}C-acetate. This tracer was originally used for measuring oxidative metabolism in the myocardium. In the brain acetate is preferentially taken up into and metabolised by glial cells. In tumour cells acetate can be transformed into acetyl-CoA, or used as a precursor of membrane fatty acids [151]. In low-grade gliomas there is little uptake of acetate; the uptake is significantly increased in high-grade gliomas, even in tumours with little FDG uptake [142, 150].

The future: imaging molecular expression

Compared to our increased understanding of the molecular biology of low grade tumours, the imaging modalities that are currently available could be considered as relatively crude. There is a lot of largely preclinical work that is trying to develop imaging methods to image gene expression. These techniques, extensively reviewed elsewhere [82, 83], mostly use reporter genes that are inserted into tumours using either cells or via viral vectors. Most studies identify gene expression using optical imaging. A recent PET study showed that it is possible to detect expression of the *Herpes simplex* thymidine kinase gene (HSV1 tk) in a patient with a glioblastoma undergoing immunotherapy using CD8$^+$ T-cell engineered to express IL-13 and the HSV1 tk gene with a ^{18}F-radiolabelled 9-[4-fluoro-3-(hydroxymethyl)butyl]guanine (^{18}F-FHBG) [149]. There is a great need for improvements in detection technology and

the development of more sensitive and specific reporters before these techniques are used in the routine clinical management of patients with low-grade gliomas.

Conclusions

Application of these new MR and PET techniques can help greatly in confirming a diagnosis, providing prognostic information, guiding biopsies and treatment. Perfusion and diffusion MR can be performed on all modern MR machines – most will also do proton spectroscopy. These are becoming standard methods of assessing low-grade gliomas in a clinical setting. The availability of PET is more limited, but the development of PET/CT and the increasing utility of this in cancer treatment will ensure that they will be available in most cancer centres and will be come in increasingly important tool in the management of these difficult tumours.

As we now begin to understand what information these imaging techniques tell us, the next stage is to use these methods to individualise treatment. Such starting points may be differentiating those tumours that are likely to progress rapidly from those that have a more indolent course. The former group may be suitable for more aggressive therapy at diagnosis. In addition, markers that provide warning of likely transformation may allow early intervention. Clinical trials are needed to determine the utility of these imaging biomarkers in a clinical setting.

Acknowledgements

I wish to thank Dr. Mary McLean from the CRUK Cambridge Research Institute for providing the MRS images.

References

1. Al Okaili RN, Krejza J, Woo JH, Wolf RL, O'Rourke DM, Judy KD, *et al.* (2007) Intraaxial brain masses: MR imaging-based diagnostic strategy – initial experience. Radiology 243(2): 539–50
2. Alavi JB, Alavi A, Chawluk J, Kushner M, Powe J, Hickey W, *et al.* (1988) Positron emission tomography in patients with glioma. A predictor of prognosis. Cancer 62(6): 1074–78
3. Alimenti A, Delavelle J, Lazeyras F, Yilmaz H, Dietrich PY, de TN, *et al.* (2007) Monovoxel ^{1}H magnetic resonance spectroscopy in the progression of gliomas. Eur Neurol 58(4): 198–209
4. Aronen HJ, Gazit IE, Louis DN, Buchbinder BR, Pardo FS, Weisskoff RM, *et al.* (1994) Cerebral blood volume maps of gliomas: comparison with tumor grade and histologic findings. Radiology 191(1): 41–51

5. Aronen HJ, Pardo FS, Kennedy DN, Belliveau JW, Packard SD, Hsu DW, *et al.* (2000) High microvascular blood volume is associated with high glucose uptake and tumor angiogenesis in human gliomas. Clin Cancer Res 6(6): 2189–200
6. Astrakas LG, Zurakowski D, Tzika AA, Zarifi MK, Anthony DC, De GU, *et al.* (2004) Noninvasive magnetic resonance spectroscopic imaging biomarkers to predict the clinical grade of pediatric brain tumors. Clin Cancer Res 10(24): 8220–28
7. Beppu T, Inoue T, Shibata Y, Kurose A, Arai H, Ogasawara K, *et al.* (2003) Measurement of fractional anisotropy using diffusion tensor MRI in supratentorial astrocytic tumours. J Neurooncol 63: 109–16
8. Boxerman JL, Hamberg LM, Rosen BR, Weisskoff RM (1995) MR contrast due to intravascular magnetic susceptibility perturbations. Magn Reson Med 34(4): 555–66
9. Boxerman JL, Schmainda KM, Weisskoff RM (2006) Relative cerebral blood volume maps corrected for contrast agent extravasation significantly correlate with glioma tumor grade, whereas uncorrected maps do not. Am J Neuroradiol 27(4): 859–67
10. Bruehlmeier M, Roelcke U, Schubiger PA, Ametamey SM (2004) Assessment of hypoxia and perfusion in human brain tumors using PET with ^{18}F-fluoromisonidazole and $^{15}H_{20}$. J Nucl Med 45(11): 1851–59
11. Bruehlmeier M, Roelcke U, Schubiger PA, Ametamey SM (2004) Assessment of hypoxia and perfusion in human brain tumors using PET with ^{18}F-fluoromisonidazole and $^{15}H_{20}$. J Nucl Med 45(11): 1851–59
12. Bulakbasi N, Kocaoglu M, Ors F, Tayfun C, Ucoz T (2003) Combination of single-voxel proton MR spectroscopy and apparent diffusion coefficient calculation in the evaluation of common brain tumors. Am J Neuroradiol 24(2): 225–33
13. Butteriss DJ, Ismail A, Ellison DW, Birchall D (2003) Use of serial proton magnetic resonance spectroscopy to differentiate low-grade glioma from tumefactive plaque in a patient with multiple sclerosis. Br J Radiol 76(909): 662–65
14. Cairncross JG, Ueki K, Zlatescu MC, Lisle DK, Finkelstein DM, Hammond RR, *et al.* (1998) Specific genetic predictors of chemotherapeutic response and survival in patients with anaplastic oligodendrogliomas. J Natl Cancer Inst 90(19): 1473–79
15. Callot V, Galanaud D, Figarella-Branger D, Lefur Y, Metellus P, Nicoli F, *et al.* (2007) Correlations between MR and endothelial hyperplasia in low-grade gliomas. J Magn Reson Imaging 26(1): 52–60
16. Cha S, Tihan T, Crawford F, Fischbein NJ, Chang S, Bollen A, *et al.* (2005) Differentiation of low-grade oligodendrogliomas from low-grade astrocytomas by using quantitative blood-volume measurements derived from dynamic susceptibility contrast-enhanced MR imaging. Am J Neuroradiol 26(2): 266–73
17. Chamberlain MC, Murovic JA, Levin VA (1988) Absence of contrast enhancement on CT brain scans of patients with supratentorial malignant gliomas. Neurology 38(9): 1371–74
18. Chan YL, Leung SF, King AD, Choi PH, Metreweli C (1999) Late radiation injury to the temporal lobes: morphologic evaluation at MR imaging. Radiology 213(3): 800–07
19. Chan YL, Yeung DK, Leung SF, Cao G (1999) Proton magnetic resonance spectroscopy of late delayed radiation-induced injury of the brain. J Magn Reson Imaging 10(2): 130–37
20. Chao ST, Suh JH, Raja S, Lee SY, Barnett G (2001) The sensitivity and specificity of FDG PET in distinguishing recurrent brain tumor from radionecrosis in patients treated with stereotactic radiosurgery. Int J Cancer 96(3): 191–97

21. Chen W, Cloughesy T, Kamdar N, Satyamurthy N, Bergsneider M, Liau L, *et al.* (2005) Imaging proliferation in brain tumors with ^{18}F-FLT PET: comparison with ^{18}F-FDG. J Nucl Med 46(6): 945–52
22. Choi SJ, Kim JS, Kim JH, Oh SJ, Lee JG, Kim CJ, *et al.* (2005) [^{18}F]3-deoxy-3-fluorothymidine PET for the diagnosis and grading of brain tumors. Eur J Nucl Med Mol Imaging 32(6): 653–59
23. Chung JK, Kim YK, Kim SK, Lee YJ, Paek S, Yeo JS, *et al.* (2002) Usefulness of ^{11}C-methionine PET in the evaluation of brain lesions that are hypo- or isometabolic on ^{18}F-FDG PET. Eur J Nucl Med Mol Imaging 29(2): 176–82
24. Danchaivijitr N, Waldman AD, Tozer DJ, Benton CE, Brasil CG, Tofts PS, *et al.* (2008) Low-grade gliomas: do changes in rCBV measurements at longitudinal perfusion-weighted MR imaging predict malignant transformation? Radiology 247(1): 170–78
25. Daumas-Duport C, Tucker ML, Kolles H, Cervera P, Beuvon F, Varlet P, *et al.* (1997) Oligodendrogliomas. Part II: A new grading system based on morphological and imaging criteria. J Neurooncol 34(1): 61–78
26. De Witte O, Goldberg I, Wikler D, Rorive S, Damhaut P, Monclus M, *et al.* (2001) Positron emission tomography with injection of methionine as a prognostic factor in glioma. J Neurosurg 95(5): 746–50
27. De Witte O, Levivier M, Violon P, Salmon I, Damhaut P, Wikler D Jr, *et al.* (1996) Prognostic value positron emission tomography with [^{18}F]fluoro-2-deoxy-D-glucose in the low-grade glioma. Neurosurgery 39(3): 470–76
28. Dean BL, Drayer BP, Bird CR, Flom RA, Hodak JA, Coons SW, *et al.* (1990) Gliomas: classification with MR imaging. Radiology 174(2): 411–15
29. Delbeke D, Meyerowitz C, Lapidus RL, Maciunas RJ, Jennings MT, Moots PL, *et al.* (1995) Optimal cutoff levels of F-18 fluorodeoxyglucose uptake in the differentiation of low-grade from high-grade brain tumors with PET. Radiology 195(1): 47–52
30. Derlon JM, Chapon F, Noel MH, Khouri S, Benali K, Petit-Taboue MC, *et al.* (2000) Non-invasive grading of oligodendrogliomas: correlation between in vivo metabolic pattern and histopathology. Eur J Nucl Med 27(7): 778–87
31. Derlon JM, Petit-Taboue MC, Chapon F, Beaudouin V, Noel MH, Creveuil C, *et al.* (1997) The in vivo metabolic pattern of low-grade brain gliomas: a positron emission tomographic study using ^{18}F-fluorodeoxyglucose and ^{11}C-L-methylmethionine. Neurosurgery 40(2): 276–87
32. Di Chiro G, Oldfield E, Wright DC, De Michele D, Katz DA, Patronas NJ, *et al.* (1988) Cerebral necrosis after radiotherapy and/or intraarterial chemotherapy for brain tumors: PET and neuropathologic studies. Am J Roentgenol 150(1): 189–97
33. Donahue KM, Krouwer HG, Rand SD, Pathak AP, Marszalkowski CS, Censky SC, *et al.* (2000) Utility of simultaneously acquired gradient-echo and spin-echo cerebral blood volume and morphology maps in brain tumor patients. Magn Reson Med 43(6): 845–53
34. Donahue KM, Krouwer HG, Rand SD, Pathak AP, Marszalkowski CS, Censky SC, *et al.* (2000) Utility of simultaneously acquired gradient-echo and spin-echo cerebral blood volume and morphology maps in brain tumor patients. Magn Reson Med 43(6): 845–53
35. Eary JF, Mankoff DA, Spence AM, Berger MS, Olshen A, Link JM, *et al.* (1999) 2-[C-11]thymidine imaging of malignant brain tumors. Cancer Res 59(3): 615–21

36. Emblem KE, Nedregaard B, Nome T, Due-Tonnessen P, Hald JK, Scheie D, *et al.* (2008) Glioma grading by using histogram analysis of blood volume heterogeneity from MR-derived cerebral blood volume maps. Radiology 247(3): 808–17
37. Fayed N, Modrego PJ (2005) The contribution of magnetic resonance spectroscopy and echoplanar perfusion-weighted MRI in the initial assessment of brain tumours. J Neurooncol 72(3): 261–65
38. Floeth FW, Pauleit D, Sabel M, Stoffels G, Reifenberger G, Riemenschneider MJ, *et al.* (2007) Prognostic value of *O*-(2-^{18}F-Fluoroethyl)-L-Tyrosine PET and MRI in low-grade glioma. J Nucl Med 48(4): 519–27
39. Fox IH, Kelley WN (1978) The role of adenosine and 2′-deoxyadenosine in mammalian cells. Annu Rev Biochem 47: 655–86
40. Gauvain KM, McKinstry RC, Mukherjee P, Perry A, Neil JJ, Kaufman BA, *et al.* (2001) Evaluating pediatric brain tumor cellularity with diffusion-tensor imaging. Am J Roentgenol 177(2): 449–54
41. Giammarile F, Cinotti LE, Jouvet A, Ramackers JM, Saint PG, Thiesse P, *et al.* (2004) High and low grade oligodendrogliomas (ODG): correlation of amino-acid and glucose uptakes using PET and histological classifications. J Neurooncol 68(3): 263–74
42. Go KG, Keuter EJ, Kamman RL, Pruim J, Metzemaekers JD, Staal MJ, *et al.* (1994) Contribution of magnetic resonance spectroscopic imaging and L-[1-^{11}C]tyrosine positron emission tomography to localization of cerebral gliomas for biopsy. Neurosurgery 34(6): 994–1002
43. Goebell E, Paustenbach S, Vaeterlein O, Ding XQ, Heese O, Fiehler J, *et al.* (2006) Low-grade and anaplastic gliomas: differences in architecture evaluated with diffusion-tensor MR imaging. Radiology 239(1): 217–22
44. Goldman S, Levivier M, Pirotte B, Brucher JM, Wikler D, Damhaut P, *et al.* (1996) Regional glucose metabolism and histopathology of gliomas: a study based on positron emission tomography-guided biopsy. Cancer 78: 1098–1106
45. Grierson JR, Schwartz JL, Muzi M, Jordan R, Krohn KA (2004) Metabolism of 3′-deoxy-3′-[F-18]fluorothymidine in proliferating A549 cells: validations for positron emission tomography. Nucl Med Biol 31(7): 829–37
46. Guillevin R, Menuel C, Duffau H, Kujas M, Capelle L, Aubert A, *et al.* (2008) Proton magnetic resonance spectroscopy predicts proliferative activity in diffuse low-grade gliomas. J Neurooncol 87(2): 181–87
47. Hara T, Kondo T, Hara T, Kosaka N (2003) Use of ^{18}F-choline and ^{11}C-choline as contrast agents in positron emission tomography imaging-guided stereotactic biopsy sampling of gliomas. J Neurosurg 99(3): 474–79
48. Hein PA, Eskey CJ, Dunn JF, Hug EB (2004) Diffusion-weighted imaging in the follow-up of treated high-grade gliomas: Tumor recurrence versus radiation injury. Am J Neuroradiol 25(2): 201–09
49. Heiss WD, Heindel W, Herholz K, Rudolf J, Bunke J, Jeske J, *et al.* (1990) Positron emission tomography of fluorine-18-deoxyglucose and image-guided phosphorus-31 magnetic resonance spectroscopy in brain tumors. J Nucl Med 31(3): 302–10
50. Herholz K, Holzer T, Bauer B, Schroder R, Voges J, Ernestus RI, *et al.* (1998) ^{11}C-methionine PET for differential diagnosis of low-grade gliomas. Neurology 50(5): 1316–22

51. Herminghaus S, Dierks T, Pilatus U, Moller-Hartmann W, Wittsack J, Marquardt G, *et al.* (2003) Determination of histopathological tumor grade in neuroepithelial brain tumors by using spectral pattern analysis of in vivo spectroscopic data. J Neurosurg 98(1): 74–81
52. Inoue T, Ogasawara K, Beppu T, Ogawa A, Kabasawa H (2005) Diffusion tensor imaging for preoperative evaluation of tumor grade in gliomas. Clin Neurol Neurosurg 107(3): 174–80
53. Isselbacher KJ (1972) Sugar and amino acid transport by cells in culture – differences between normal and malignant cells. N Engl J Med 286(17): 929–33
54. Jacobs AH, Thomas A, Kracht LW, Li H, Dittmar C, Garlip G, *et al.* (2005) ^{18}F-Fluoro-L-Thymidine and ^{11}C-Methylmethionine as markers of increased transport and proliferation in brain tumors. J Nucl Med 46(12): 1948–58
55. Jenkinson MD, du Plessis DG, Smith TS, Joyce KA, Warnke PC, Walker C (2006) Histological growth patterns and genotype in oligodendroglial tumours: correlation with MRI features. Brain 129(Pt 7): 1884–91
56. Jenkinson MD, Smith TS, Brodbelt AR, Joyce KA, Warnke PC, Walker C (2007) Apparent diffusion coefficients in oligodendroglial tumors characterized by genotype. J Magn Reson Imaging 26(6): 1405–12
57. Jenkinson MD, Smith TS, Joyce K, Fildes D, du Plessis DG, Warnke PC, *et al.* (2005) MRS of oligodendroglial tumors: correlation with histopathology and genetic subtypes. Neurology 64(12): 2085–89
58. Jenkinson MD, Smith TS, Joyce KA, Fildes D, Broome J, du Plessis DG, *et al.* (2006) Cerebral blood volume, genotype and chemosensitivity in oligodendroglial tumours. Neuroradiology 48(10): 703–13
59. Kim S, Chung JK, Im SH, Jeong JM, Lee DS, Kim DG, *et al.* (2005) ^{11}C-methionine PET as a prognostic marker in patients with glioma: comparison with ^{18}F-FDG PET. Eur J Nucl Med Mol Imaging 32(1): 52–59
60. Kim S, Chung JK, Im SH, Jeong JM, Lee DS, Kim DG, *et al.* (2005) ^{11}C-methionine PET as a prognostic marker in patients with glioma: comparison with ^{18}F-FDG PET. Eur J Nucl Med Mol Imaging 32(1): 52–59
61. Kleihues P, Cavenee WK (2000) Pathology and genetics of tumours of the nervous system. IARC Press, Lyon, France
62. Knopp EA, Cha S, Johnson G, Mazumdar A, Golfinos JG, Zagzag D, *et al.* (1999) Glial neoplasms: dynamic contrast-enhanced T_2*-weighted MR imaging. Radiology 211(3): 791–98
63. Kondziolka D, Lunsford LD, Martinez AJ (1993) Unreliability of contemporary neurodiagnostic imaging in evaluating suspected adult supratentorial (low-grade) astrocytoma. J Neurosurg 79(4): 533–36
64. Kong XB, Zhu QY, Vidal PM, Watanabe KA, Polsky B, Armstrong D, *et al.* (1992) Comparisons of anti-human immunodeficiency virus activities, cellular transport, and plasma and intracellular pharmacokinetics of 3′-fluoro-3′-deoxythymidine and 3′-azido-3′-deoxythymidine. Antimicrob Agents Chemother 36(4): 808–18
65. Kono K, Inoue Y, Nakayama K, Shakudo M, Morino M, Ohata K, *et al.* (2001) The role of diffusion-weighted imaging in patients with brain tumors. Am J Neuroradiol 22(6): 1081–88

66. Kuwert T, Probst-Cousin S, Woesler B, Morgenroth C, Lerch H, Matheja P, *et al.* (1997) Iodine-123-alpha-methyl tyrosine in gliomas: correlation with cellular density and proliferative activity. J Nucl Med 38(10): 1551–55
67. Lam WW, Poon WS, Metreweli C (2002) Diffusion MR imaging in glioma: does it have any role in the pre-operation determination of grading of glioma? Clin Radiol 57(3): 219–25
68. Law M, Brodsky JE, Babb J, Rosenblum M, Miller DC, Zagzag D, *et al.* (2007) High cerebral blood volume in human gliomas predicts deletion of chromosome 1p: preliminary results of molecular studies in gliomas with elevated perfusion. J Magn Reson Imaging 25(6): 1113–19
69. Law M, Oh S, Johnson G, Babb JS, Zagzag D, Golfinos J, *et al.* (2006) Perfusion magnetic resonance imaging predicts patient outcome as an adjunct to histopathology: a second reference standard in the surgical and nonsurgical treatment of low-grade gliomas. Neurosurgery 58(6): 1099–1107
70. Law M, Yang S, Babb JS, Knopp EA, Golfinos JG, Zagzag D, *et al.* (2004) Comparison of cerebral blood volume and vascular permeability from dynamic susceptibility contrast-enhanced perfusion MR imaging with glioma grade. Am J Neuroradiol 25(5): 746–55
71. Law M, Yang S, Wang H, Babb JS, Johnson G, Cha S, *et al.* (2003) Glioma grading: sensitivity, specificity, and predictive values of perfusion MR imaging and proton MR spectroscopic imaging compared with conventional MR imaging. Am J Neuroradiol 24(10): 1989–98
72. Law M, Young R, Babb J, Pollack E, Johnson G (2007) Histogram analysis versus region of interest analysis of dynamic susceptibility contrast perfusion MR imaging data in the grading of cerebral gliomas. Am J Neuroradiol 28(4): 761–66
73. Law M, Young RJ, Babb JS, Peccerelli N, Chheang S, Gruber ML, *et al.* (2008) Gliomas: predicting time to progression or survival with cerebral blood volume measurements at dynamic susceptibility-weighted contrast-enhanced perfusion MR imaging. Radiology 247(2): 490–98
74. Lee YY, Van TP (1989) Intracranial oligodendrogliomas: imaging findings in 35 untreated cases. Am J Roentgenol 152(2): 361–69
75. Lev MH, Ozsunar Y, Henson JW, Rasheed AA, Barest GD, Harsh GR, *et al.* (2004) Glial tumor grading and outcome prediction using dynamic spin-echo MR susceptibility mapping compared with conventional contrast-enhanced MR: confounding effect of elevated rCBV of oligodendrogliomas. Am J Neuroradiol 25(2): 214–21
76. Levivier M, Goldman S, Pirotte B, Brucher JM, Baleriaux D, Luxen A, *et al.* (1995) Diagnostic yield of stereotactic brain biopsy guided by positron emission tomography with [^{18}F]fluorodeoxyglucose. J Neurosurg 82(3): 445–52
77. Maia AC, Malheiros SM, da Rocha AJ, da Silva CJ, Gabbai AA, Ferraz FA, *et al.* (2005) MR cerebral blood volume maps correlated with vascular endothelial growth factor expression and tumor grade in nonenhancing gliomas. Am J Neuroradiol 26(4): 777–83
78. Maia AC, Malheiros SM, da Rocha AJ, Stavale JN, Guimaraes IF, Borges LR, *et al.* (2004) Stereotactic biopsy guidance in adults with supratentorial nonenhancing gliomas: role of perfusion-weighted magnetic resonance imaging. J Neurosurg 101(6): 970–76
79. Maintz D, Heindel W, Kugel H, Jaeger R, Lackner KJ (2002) Phosphorus-31 MR spectroscopy of normal adult human brain and brain tumours. NMR Biomed 15(1): 18–27

80. Mandonnet E, Delattre JY, Tanguy ML, Swanson KR, Carpentier AF, Duffau H, *et al.* (2003) Continuous growth of mean tumor diameter in a subset of grade II gliomas. Ann Neurol 53(4): 524–28
81. Massager N, David P, Goldman S, Pirotte B, Wikler D, Salmon I, *et al.* (2000) Combined magnetic resonance imaging- and positron emission tomography-guided stereotactic biopsy in brainstem mass lesions: diagnostic yield in a series of 30 patients. J Neurosurg 93(6): 951–57
82. Massoud TF, Singh A, Gambhir SS (2008) Noninvasive molecular neuroimaging using reporter genes: part I, principles revisited. Am J Neuroradiol 29(2): 229–34
83. Massoud TF, Singh A, Gambhir SS (2008) Noninvasive molecular neuroimaging using reporter genes. Part II: Experimental, current, and future applications. Am J Neuroradiol 29(3): 409–18
84. McBride DQ, Miller BL, Nikas DL, Buchthal S, Chang L, Chiang F, *et al.* (1995) Analysis of brain tumors using ^{1}H magnetic resonance spectroscopy. Surg Neurol 44(2): 137–44
85. McKnight TR, dem Bussche MH, Vigneron DB, Lu Y, Berger MS, McDermott MW, *et al.* (2002) Histopathological validation of a three-dimensional magnetic resonance spectroscopy index as a predictor of tumor presence. J Neurosurg 97(4): 794–802
86. McKnight TR, Lamborn KR, Love TD, Berger MS, Chang S, Dillon WP, *et al.* (2007) Correlation of magnetic resonance spectroscopic and growth characteristics within Grades II and III gliomas. J Neurosurg 106(4): 660–66
87. Megyesi JF, Kachur E, Lee DH, Zlatescu MC, Betensky RA, Forsyth PA, *et al.* (2004) Imaging correlates of molecular signatures in oligodendrogliomas. Clin Cancer Res 10(13): 4303–06
88. Meyerand ME, Pipas JM, Mamourian A, Tosteson TD, Dunn JF (1999) Classification of biopsy-confirmed brain tumors using single-voxel MR spectroscopy. Am J Neuroradiol 20(1): 117–23
89. Mineura K, Sasajima T, Kowada M, Ogawa T, Hatazawa J, Uemura K (1996) Long-term positron emission tomography evaluation of slowly progressive gliomas. Eur J Cancer 32A(7): 1257–60
90. Moller-Hartmann W, Herminghaus S, Krings T, Marquardt G, Lanfermann H, Pilatus U, *et al.* (2002) Clinical application of proton magnetic resonance spectroscopy in the diagnosis of intracranial mass lesions. Neuroradiology 44(5): 371–81
91. Moritani T, Ekholm S, Westesson P-L, Hiwatashi A (2005) Brain neoplasms. In: Moritani T, Ekholm S, Westesson P-L (eds) Diffusion-weighted MR imaging of the brain. Springer, Berlin Heidelberg, pp 161–80
92. Munch-Petersen B, Cloos L, Tyrsted G, Eriksson S (1991) Diverging substrate specificity of pure human thymidine kinases 1 and 2 against antiviral dideoxynucleosides. J Biol Chem 266(14): 9032–38
93. Murphy M, Loosemore A, Clifton AG, Howe FA, Tate AR, Cudlip SA, *et al.* (2002) The contribution of proton magnetic resonance spectroscopy (^{1}H MRS) to clinical brain tumour diagnosis. Br J Neurosurg 16(4): 329–34
94. Murphy PS, Viviers L, Abson C, Rowland IJ, Brada M, Leach MO, *et al.* (2004) Monitoring temozolomide treatment of low-grade glioma with proton magnetic resonance spectroscopy. Br J Cancer 90(4): 781–86
95. Muti M, Aprile I, Principi M, Italiani M, Guiducci A, Giulianelli G, *et al.* (2002) Study on the variations of the apparent diffusion coefficient in areas of solid tumor in high-grade gliomas. Magn Reson Imaging 20(9): 635–41

96. Muzi M, Vesselle H, Grierson JR, Mankoff DA, Schmidt RA, Peterson L, *et al.* (2005) Kinetic analysis of 3′-deoxy-3′-fluorothymidine PET studies: validation studies in patients with lung cancer. J Nucl Med 46(2): 274–82
97. Nafe R, Herminghaus S, Raab P, Wagner S, Pilatus U, Schneider B, *et al.* (2003) Preoperative proton-MR spectroscopy of gliomas – correlation with quantitative nuclear morphology in surgical specimen. J Neurooncol 63(3): 233–45
98. Negendank WG, Sauter R, Brown TR, Evelhoch JL, Falini A, Gotsis ED, *et al.* (1996) Proton magnetic resonance spectroscopy in patients with glial tumors: a multicenter study. J Neurosurg 84(3): 449–58
99. Nuutinen J, Sonninen P, Lehikoinen P, Sutinen E, Valavaara R, Eronen E, *et al.* (2000) Radiotherapy treatment planning and long-term follow-up with [(11)C]methionine PET in patients with low-grade astrocytoma. Int J Radiat Oncol Biol Phys 48(1): 43–52
100. Ogawa T, Inugami A, Hatazawa J, Kanno I, Murakami M, Yasui N, *et al.* (1996) Clinical positron emission tomography for brain tumors: comparison of fludeoxyglucose F 18 and L-methyl-^{11}C-methionine. Am J Neuroradiol 17(2): 345–53
101. Ogawa T, Shishido F, Kanno I, Inugami A, Fujita H, Murakami M, *et al.* (1993) Cerebral glioma: evaluation with methionine PET. Radiology 186(1): 45–53
102. Padhani AR, Krohn KA, Lewis JS, Alber M (2007) Imaging oxygenation of human tumours. Eur Radiol 17(4): 861–72
103. Pallud J, Mandonnet E, Duffau H, Kujas M, Guillevin R, Galanaud D, *et al.* (2006) Prognostic value of initial magnetic resonance imaging growth rates for World Health Organization Grade II gliomas. Ann Neurol 60(3): 380–83
104. Patronas NJ, Brooks RA, DeLaPaz RL, Smith BH, Kornblith PL, Di Chiro G (1983) Glycolytic rate (PET) and contrast enhancement (CT) in human cerebral gliomas. Am J Neuroradiol 4(3): 533–35
105. Patronas NJ, Di Chiro G, Kufta C, Bairamian D, Kornblith PL, Simon R, *et al.* (1985) Prediction of survival in glioma patients by means of positron emission tomography. J Neurosurg 62(6): 816–22
106. Pena A, Green HAL, Carpenter TA, Price SJ, Pickard JD, Gillard JH (2006) Enhanced visualization and quantification of magnetic resonance diffusion tensor imaging using the p:q tensor decomposition. Br J Radiol 79(938): 101–09
107. Pirotte B, Goldman S, Dewitte O, Massager N, Wikler D, Lefranc F, *et al.* (2006) Integrated positron emission tomography and magnetic resonance imaging-guided resection of brain tumors: a report of 103 consecutive procedures. J Neurosurg 104(2): 238–53
108. Pirotte B, Goldman S, Massager N, David P, Wikler D, Lipszyc M, *et al.* (2004) Combined use of ^{18}F-fluorodeoxyglucose and ^{11}C-methionine in 45 positron emission tomography-guided stereotactic brain biopsies. J Neurosurg 101(3): 476–83
109. Pirotte B, Goldman S, Salzberg S, Wikler D, David P, Vandesteene A, *et al.* (2003) Combined positron emission tomography and magnetic resonance imaging for the planning of stereotactic brain biopsies in children: experience in 9 cases. Pediatr Neurosurg 38(3): 146–55
110. Price SJ (2007) The role of advanced MR imaging in understanding brain tumour pathology. Br J Neurosurg 21(6): 562–75
111. Price SJ, Burnet NG, Donovan T, Green HA, Pena A, Antoun NM, *et al.* (2003) Diffusion tensor imaging of brain tumours at 3T: a potential tool for assessing white matter tract invasion? Clin Radiol 58(6): 455–62

112. Price SJ, Fryer TD, Cleij MC, Dean AF, Joseph J, Salvador R, *et al.* (2008) Imaging regional variation of cellular proliferation in gliomas using 3′-deoxy-3′-[^{18}F]fluorothymidine positron-emission tomography: an image-guided biopsy study. Clin Radiol [Epub ahead of print]:-doi:10.1016/j.crad.2008.01.016
113. Price SJ, Jena R, Burnet NG, Hutchinson PJ, Dean AF, Pena A, *et al.* (2006) Improved delineation of glioma margins and regions of infiltration with the use of diffusion tensor imaging: an image-guided biopsy study. Am J Neuroradiol 27(9): 1969–74
114. Price SJ, Pena A, Burnet NG, Jena R, Green HA, Carpenter TA, *et al.* (2004) Tissue signature characterisation of diffusion tensor abnormalities in cerebral gliomas. Eur Radiol 14(10): 1909–17
115. Recht LD, Lew R, Smith TW (1992) Suspected low-grade glioma: is deferring treatment safe? Ann Neurol 31(4): 431–36
116. Reijneveld JC, van der GJ, Ramos LM, Bromberg JE, Taphoorn MJ (2005) Proton MRS imaging in the follow-up of patients with suspected low-grade gliomas. Neuroradiology 47(12): 887–91
117. Ribom D, Eriksson A, Hartman M, Engler H, Nilsson A, Langstrom B, *et al.* (2001) Positron emission tomography (11)C-methionine and survival in patients with low-grade gliomas. Cancer 92(6): 1541–49
118. Ribom D, Smits A (2005) Baseline ^{11}C-methionine PET reflects the natural course of grade 2 oligodendrogliomas. Neurol Res 27(5): 516–21
119. Rock JP, Hearshen D, Scarpace L, Croteau D, Gutierrez J, Fisher JL, *et al.* (2002) Correlations between magnetic resonance spectroscopy and image-guided histopathology, with special attention to radiation necrosis. Neurosurgery 51(4): 912–20
120. Rock JP, Scarpace L, Hearshen D, Gutierrez J, Fisher JL, Rosenblum M, *et al.* (2004) Associations among magnetic resonance spectroscopy, apparent diffusion coefficients, and image-guided histopathology with special attention to radiation necrosis. Neurosurgery 54(5): 1111–19
121. Roelcke U, von Ammon K, Hausmann O, Kaech DL, Vanloffeld W, Landolt H, *et al.* (1999) Operated low grade astrocytomas: a long term PET study on the effect of radiotherapy. J Neurol Neurosurg Psychiatry 66(5): 644–47
122. Saga T, Kawashima H, Araki N, Takahashi JA, Nakashima Y, Higashi T, *et al.* (2006) Evaluation of primary brain tumors with FLT-PET: usefulness and limitations. Clin Nucl Med 31(12): 774–80
123. Scott JN, Brasher PMA, Sevick RJ, Rewcastle NB, Forsyth PA (2002) How often are nonenhancing supratentorial gliomas malignant? A population study. Neurology 59(6): 947–49
124. Setzer M, Herminghaus S, Marquardt G, Tews DS, Pilatus U, Seifert V, *et al.* (2007) Diagnostic impact of proton MR-spectroscopy versus image-guided stereotactic biopsy. Acta Neurochir (Wien) 149(4): 379–86
125. Shields AF, Grierson JR, Dohmen BM, Machulla HJ, Stayanoff JC, Lawhorn-Crews JM, *et al.* (1998) Imaging proliferation in vivo with [F-18]FLT and positron emission tomography. Nat Med 4(11): 1334–36
126. Shin JH, Lee HK, Kwun BD, Kim JS, Kang W, Choi CG, *et al.* (2002) Using relative cerebral blood flow and volume to evaluate the histopathologic grade of cerebral gliomas: preliminary results. Am J Roentgenol 179(3): 783–89

127. Sijens PE, Heesters MA, Enting RH, van der Graaf WT, Potze JH, Irwan R, *et al.* (2007) Diffusion tensor imaging and chemical shift imaging assessment of heterogeneity in low-grade glioma under temozolomide chemotherapy. Cancer Invest 25(8): 706–710
128. Sijens PE, Oudkerk M (2002) ^{1}H chemical shift imaging characterization of human brain tumor and edema. Eur Radiol 12(8): 2056–61
129. Spampinato MV, Smith JK, Kwock L, Ewend M, Grimme JD, Camacho DL, *et al.* (2007) Cerebral blood volume measurements and proton MR spectroscopy in grading of oligodendroglial tumors. Am J Roentgenol 188(1): 204–12
130. Stockhammer F, Thomale UW, Plotkin M, Hartmann C, Von DA (2007) Association between fluorine-18-labeled fluorodeoxyglucose uptake and 1p and 19q loss of heterozygosity in World Health Organization Grade II gliomas. J Neurosurg 106(4): 633–37
131. Sugahara T, Korogi Y, Kochi M, Ikushima I, Hirai T, Okuda T, *et al.* (1998) Correlation of MR imaging-determined cerebral blood volume maps with histologic and angiographic determination of vascularity of gliomas. Am J Roentgenol 171(6): 1479–86
132. Sugahara T, Korogi Y, Kochi M, Ikushima I, Shigematu Y, Hirai T, *et al.* (1999) Usefulness of diffusion-weighted MRI with echo-planar technique in the evaluation of cellularity in gliomas. J Magn Reson Imaging 9(1): 53–60
133. Sugahara T, Korogi Y, Kochi M, Ushio Y, Takahashi M (2001) Perfusion-sensitive MR imaging of gliomas: comparison between gradient-echo and spin-echo echo-planar imaging techniques. Am J Neuroradiol 22(7): 1306–15
134. Sugahara T, Korogi Y, Tomiguchi S, Shigematsu Y, Ikushima I, Kira T, *et al.* (2000) Posttherapeutic intraaxial brain tumor: the value of perfusion-sensitive contrast-enhanced MR imaging for differentiating tumor recurrence from nonneoplastic contrast-enhancing tissue. Am J Neuroradiol 21(5): 901–09
135. Sundgren PC, Fan X, Weybright P, Welsh RC, Carlos RC, Petrou M, *et al.* (2006) Differentiation of recurrent brain tumor versus radiation injury using diffusion tensor imaging in patients with new contrast-enhancing lesions. Magn Reson Imaging 24(9): 1131–42
136. Tamura M, Shibasaki T, Zama A, Kurihara H, Horikoshi S, Ono N, *et al.* (1998) Assessment of malignancy of glioma by positron emission tomography with ^{18}F-fluorodeoxyglucose and single photon emission computed tomography with thallium-201 chloride. Neuroradiology 40(4): 210–15
137. Tate AR, Underwood J, Acosta DM, Julia-Sape M, Majos C, Moreno-Torres A, *et al.* (2006) Development of a decision support system for diagnosis and grading of brain tumours using in vivo magnetic resonance single voxel spectra. NMR Biomed 19(4): 411–34
138. Tedeschi G, Lundbom N, Raman R, Bonavita S, Duyn JH, Alger JR, *et al.* (1997) Increased choline signal coinciding with malignant degeneration of cerebral gliomas: a serial proton magnetic resonance spectroscopy imaging study. J Neurosurg 87(4): 516–24
139. Thiel A, Pietrzyk U, Sturm V, Herholz K, Hovels M, Schroder R (2000) Enhanced accuracy in differential diagnosis of radiation necrosis by positron emission tomography-magnetic resonance imaging coregistration: technical case report. Neurosurgery 46(1): 232–34
140. Tofts PS, Benton CE, Weil RS, Tozer DJ, Altmann DR, Jager HR, *et al.* (2007) Quantitative analysis of whole-tumor Gd enhancement histograms predicts malignant transformation in low-grade gliomas. J Magn Reson Imaging 25(1): 208–14
141. Tozer DJ, Jager HR, Danchaivijitr N, Benton CE, Tofts PS, Rees JH, *et al.* (2007) Apparent diffusion coefficient histograms may predict low-grade glioma subtype. NMR Biomed 20(1): 49–57

142. Tsuchida T, Takeuchi H, Okazawa H, Tsujikawa T, Fujibayashi Y (2008) Grading of brain glioma with 1-^{11}C-acetate PET: comparison with ^{18}F-FDG PET. Nucl Med Biol 35(2): 171–76
143. Tsui EY, Chan JH, Leung TW, Yuen MK, Cheung YK, Luk SH, *et al.* (2000) Radionecrosis of the temporal lobe: dynamic susceptibility contrast MRI. Neuroradiology 42(2): 149–52
144. Valk PE, Mathis CA, Prados MD, Gilbert JC, Budinger TF (1992) Hypoxia in human gliomas: demonstration by PET with fluorine-18-fluoromisonidazole. J Nucl Med 33(12): 2133–37
145. Van Laere K, Ceyssens S, Van Calenbergh F, de Groot T, Menten J, Flamen P, *et al.* (2005) Direct comparison of ^{18}F-FDG and ^{11}C-methionine PET in suspected recurrence of glioma: sensitivity, inter-observer variability and prognostic value. Eur J Nucl Med Mol Imaging 32(1): 39–51
146. Vuori K, Kankaanranta L, Hakkinen AM, Gaily E, Valanne L, Granstrom ML, *et al.* (2004) Low-grade gliomas and focal cortical developmental malformations: differentiation with proton MR spectroscopy. Radiology 230(3): 703–08
147. Warburg O (1956) On the origin of cancer cells. Science 123(3191): 309–14
148. White ML, Zhang Y, Kirby P, Ryken TC (2005) Can tumor contrast enhancement be used as a criterion for differentiating tumor grades of oligodendrogliomas? Am J Neuroradiol 26(4): 784–90
149. Yaghoubi SS, Jensen MC, Satyamurthy N, Budhiraja S, Paik D, Czernin J, *et al.* (2009) Noninvasive detection of therapeutic cytolytic T cells with ^{18}F-FHBG PET in a patient with glioma. Nat Clin Prac Oncol 6(1): 53–58
150. Yamamoto Y, Nishiyama Y, Kimura N, Kameyama R, Kawai N, Hatakeyama T, *et al.* (2008) (11)C-Acetate PET in the evaluation of brain glioma: comparison with (11)C-Methionine and (18)F-FDG-PET. Mol Imaging Biol, Jun 10 [Epub ahead of print]
151. Yoshimoto M, Waki A, Yonekura Y, Sadato N, Murata T, Omata N, *et al.* (2001) Characterization of acetate metabolism in tumor cells in relation to cell proliferation: acetate metabolism in tumor cells. Nucl Med Biol 28(2): 117–22